RSC Advances

This is an *Accepted Manuscript*, which has been through the Royal Society of Chemistry peer review process and has been accepted for publication.

Accepted Manuscripts are published online shortly after acceptance, before technical editing, formatting and proof reading. Using this free service, authors can make their results available to the community, in citable form, before we publish the edited article. This *Accepted Manuscript* will be replaced by the edited, formatted and paginated article as soon as this is available.

You can find more information about *Accepted Manuscripts* in the Information for Authors.

Please note that technical editing may introduce minor changes to the text and/or graphics, which may alter content. The journal's standard Terms & Conditions and the Ethical guidelines still apply. In no event shall the Royal Society of Chemistry be held responsible for any errors or omissions in this *Accepted Manuscript* or any consequences arising from the use of any information it contains.

ROYAL SOCIETY OF CHEMISTRY

www.rsc.org/advances

Please do not adjust margins

Journal Name

COMMUNICATION

Rapid template-free synthesis of air-stable hierarchical copper nanoassembly as reusable catalyst for 4-nitrophenol reduction

Received 00th January 20xx,
Accepted 00th January 20xx

DOI: 10.1039/x0xx00000x

www.rsc.org/

Sourav Ghosh,[a] Rituparna Das,[a] Ipsita Hazra Chowdhury,[a] Piyali Bhanja[b] and Milan Kanti Naskar[a*]

Hierarchical copper nanoassembly was synthesized by one-pot solvothermal treatment at 150 °C/2h in the presence of copper nitrate, formamide and water. The product exhibited phase pure hierarchical Cu microspheroid (2-7 µm) comprising of nanorod (50-100 nm) assembly. The Cu microspheroid showed excellent air-stability, antioxidative property and catalytic reduction of p-nitrophenol.

Copper nanostructures have drawn fascinating attention in recent times due to its relatively low cost and large abundance compared to gold or silver, while still being relatively noble. They are well-known for their catalytic, optical, electronic and antimicrobial[1-4] applications. Synthesis of copper nanostructure has been reported by different methods like reverse micelle,[5-7] chemical reduction,[8] polyol,[9] electrochemical[10] and sonochemical[11] etc. Recently, Miranda *et al.* have reported laser-ablation method for copper nanoparticle.[12] Dar *et al.* prepared air-stable copper nanostructures by surfactant-free microwave method.[13] Lam *et al.* designed copper hollow nanosphere using template-free nano-wrapping technique.[14] Liquid-phase reduction technology is conventional process for fabrication of copper nanostructures using various reducing agent such as sodium borohydride,[15] hydrazine,[16] carbohydrates,[17] formaldehyde,[18] sodium hypophosphite,[19] octadecylamine[20] etc. Recently, Kawasaki *et al.* have synthesized 2 nm copper nanocrystals based on microwave assisted polyol method.[21] Wei *et al.* reported synthesis of copper nanoparticles by decomposition of acetylacetonate precursors.[22] Nitrophenol and its derivatives, common by-products of pesticides, herbicides and synthetic dye industry, are well-known as industrial water pollutant. The p-nitrophenol (4-NP) is a water-pollutant present in industrial effluents, while p-aminophenol (4-AP) is used in drug industry, photographic developer, corrosion inhibitor etc. Among the various strategies for 4-NP deletion from environment, catalytic reduction of 4-NP to 4-AP has attracted significantly in current times.[23-28]

It is well-known that in several catalytic processes Cu_2O and/or CuO are the active species.[29,30] However, there is few reports on Cu nanoparticles as catalyst due to their susceptibility to oxidation.[13] The oxidation of Cu is enhanced with reduction in particle size. Therefore, stabilization of metallic Cu nanostructures in air is challenging toward their catalytic applications. It is worth mentioning that instead of larger surface area of nanoparticles (NPs) supported catalysts, they have some limitation in catalytic applications in terms of agglomeration at large loadings, tendency to react with supporting oxides at elevated temperature, and cumbersome processing routes.[31,32] Keeping these views in mind, in the present study, we have approached for the preparation of air stable unsupported Cu nanostructures toward their catalytic application in 4-NP reduction.

In this present communication, we report a template-free synthesis of copper nanoassembly by rapid autoclaving method at 150°C for a shorter period of time (2h) in the presence of copper nitrate, water and formamide without any post-synthetic heat treatment. Formamide played a deliberate role as weak coordinating solvent as well as a source of reducing agent in controlling the particle architectures. Thermal behavior of copper nanoassembly was also studied to perceive antioxidative properties. To the best of our knowledge, synthesis of air-stable copper nanostructure using formamide as a source of reducing agent by rapid autoclaving method has been reported for the first time. The present method of fabrication air-stable copper nanostructures is important in terms of cost-effectiveness, template free and low processing time method. Catalytic performance of the synthesized products was studied for the reduction of 4-NP to 4-AP in the presence of sodium borohydride ($NaBH_4$) at room temperature (25°C).

All reagents were analytical grade and used without further purification. In a typical experiment, 10 mmol **$Cu(NO_3)_2.3H_2O$** was dissolved in 10 mL of deionized (DI) water under stirring

[a,a]*Sol-Gel Division, CSIR-Central Glass and Ceramic Research Institute, Kolkata 700 032, India;* [b]***Indian Association for the Cultivation of Science, Kolkata 700032.***

**Corresponding author. E-mail: milan@cgcri.res.in, Fax: +91 33 24730957*

†Electronic Supplementary Information (ESI) available: [details of any supplementary information available should be included here]. See DOI: 10.1039/x0xx00000x

RSC Advances Accepted Manuscript

for 30 min at room temperature. 200 mmol of formamide was added dropwise into the former solution. The mix solution was allowed to stir for 30 min to obtain a homogeneous solution. The above solution was transferred into a 35 mL Teflon-lined autoclave followed by hydrothermal reaction at 150°C for 2 h. After the reaction, the particles were collected by centrifugation and washed with ethanol followed by drying at room temperature overnight.

X-ray diffraction (XRD) studies of the as-prepared samples were performed by Philips X'Pert Pro PW 3050/60 powder diffractometer using Ni-filtered Cu-K_α radiation (λ = 0.15418 nm) operating at 40 kV and 30 mA. X-ray photoemission spectroscopy (XPS) measurements were carried out in a PHI 5000 Versaprobe II Scanning XPS microprobe manufactured by ULVAC-PHI, USA. The spectra were recorded with monochromatic Al Kα ($h\nu$ = 1486.6 eV) radiation with an overall energy resolution of ~ 0.7 eV. H_2-TPR experiments were carried out in the temperature range of 25 to 750 ^oC using Micromeritics Chemisorb 2720 instrument, under H_2 atmosphere. In a typical experiment 245 mg of sample was placed in a U-type quartz cell followed by purging with helium gas throughout the sample for 3 h. it was cooled down to room temperature followed by purging with reducing gas (5% H_2 + 95% Argon) at flow rate of 30 mLmin^{-1} for saturation. The H_2-TPR profile of the sample was acquired using thermal conductivity detector (TCD) by elevating the temperature at 5 °C ramp per minute.[33] The thermal behaviors of the as-prepared powders were studied by thermogravimetry (TG) and differential thermal analysis (DTA) (Netzsch STA 449C, Germany) from room temperature to 600^{o}C in air atmosphere at the heating rate of 10°Cmin^{-1}. The morphology of the particles was examined by field emission scanning electron microscopy, FESEM with Zeiss, Supra^{TM} 35VP instrument operating with an accelerating voltage of 10 kV, and transmission electron microscopy, TEM using a Tecnai G2 30ST (FEI) instrument operating at 300 kV. Nitrogen adsorption-desorption measurements were conducted at 77 K with a Quantachrome (ASIQ MP) instrument.

For catalytic study, desired amount of the catalyst sample was introduced in a reaction mixture containing 0.1 mL of 3.0 x 10^{-3} M of 4-NP, 2.8 mL of water, 0.1 mL of 3.0 x 10^{-1} M $NaBH_4$ solutions at room temperature (25°C). The molar ratio of 4-NP: $NaBH_4$ was 1:10^2. The progress of catalytic performance was evaluated by the adsorption spectra at 400 nm for the decay of 4-NP peak using UV-visible-NIR spectrophotometer (V-730/730 BIO, JASCO) in the wavelength range of 250 to 500 nm. As the concentration of $NaBH_4$ was employed in excess, the reaction was considered to be a pseudo-first order, and the apparent rate constant (K_{app}) was estimated by plotting the – ln (A_t/A_0) vs time. To check the recyclability of the catalyst, the sample was washed with DI water, and dried at room temperature. Then the catalyst was ready to re-use for next time.

Figure 1 shows the XRD patterns of (a) the as-prepared Cu and (b) the same sample after exposure in open air for 12 months. The crystalline peaks at 2θ = 43.29°, 50.43°, 74.13° for both the samples were assigned to (111), (200) and (220) lattice planes

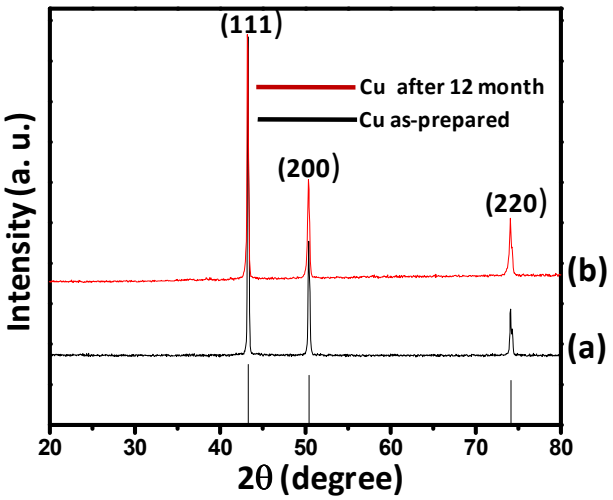

Fig. 1: XRD patterns of (a) the as-prepared Cu, and (b) the same sample after exposure in open air for 12 months

respectively of face-centered cubic (fcc) Cu (JCPDS No. 04-0836). For all the cases, the diffraction peaks of other possible impurities such as Cu_2O and CuO could not be detected. It signified that the as-prepared phase pure metallic Cu retained intact even after 12 months of open air exposure. It indicated excellent oxidation resistance of as-prepared Cu obtained *via* one-pot solvothermal treatment at 150 °C for a shorter period of time (2h) without any post-synthetic heat treatment. Chemical composition and chemical state of the as-prepared dried sample were studied by high-resolution XPS.

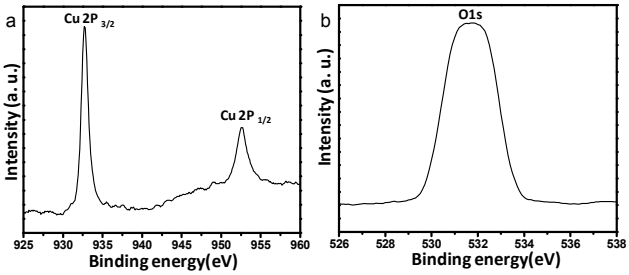

Fig. 2: reveals XPS spectra of (a) Cu 2p and (b) O1s of as-prepared Cu.

Figure 2 reveals XPS spectra of (a) Cu 2p and (b) O1s of as-prepared Cu. Major contribution from Cu $2p_{3/2}$ at 932.68 eV and Cu $2p_{1/2}$ at 952.59 eV confirmed the presence of zero valent copper.[21] From O1s spectrum, high binding energy component at 531.6 eV could be a good agreement with the presence of a hydroxyl group.[34] The outermost surface of as-prepared sample indicated no impurity of divalent Cu (530.4 eV) from O1s spectrum.[35] Combining both the Cu 2p and O1s spectra, it is attributed that the as-prepared sample was zero valent Cu in the absence of its oxidized forms. Comparing the spectral characteristics with the commercial Cu_2O and CuO,[36] absence of two main peaks at 954 eV ($Cu2p_{1/2}$) and 934 eV ($Cu2p_{3/2}$) along with shake-up satellite peaks centered at ~ 943 eV confirmed the absence of CuO in the as-prepared **sample.**

RSC Advances Accepted Manuscript

This journal is © The Royal Society of Chemistry 20xx

From O1s spectrum, the possibility of Cu_2O formation in the sample could be completely eliminated due to absence of lower energy peak at 530.3 eV.[37] However, to confirm the phase pure metallic Cu in the sample, and to determine different oxidation states of Cu in the reference oxides (Cu_2O and CuO), H_2-TPR experiments were performed. Figure S1, ESI shows the H_2-TPR profiles of as-prepared Cu, and commercial Cu_2O and CuO as reference materials. It is seen that large H_2 consumption peak was located at around 453°C for Cu_2O,[38] whereas a very weak peak appeared at around 188°C for as-prepared Cu sample. However, reference CuO shows major reduction peak at around 478°C.[39,40] The H_2 consumption peak at relatively lower temperature (188°C) for as-prepared Cu could be assigned to the reduction of dispersed Cu^{2+} species on the metallic Cu catalyst surface to metallic Cu.[41] From H_2-TPR studies, it was confirmed that the as-prepared Cu particles could contain a small amount of Cu^{2+} species on their surface, revealing lower reduction temperature compared to that found in the reference copper oxides.

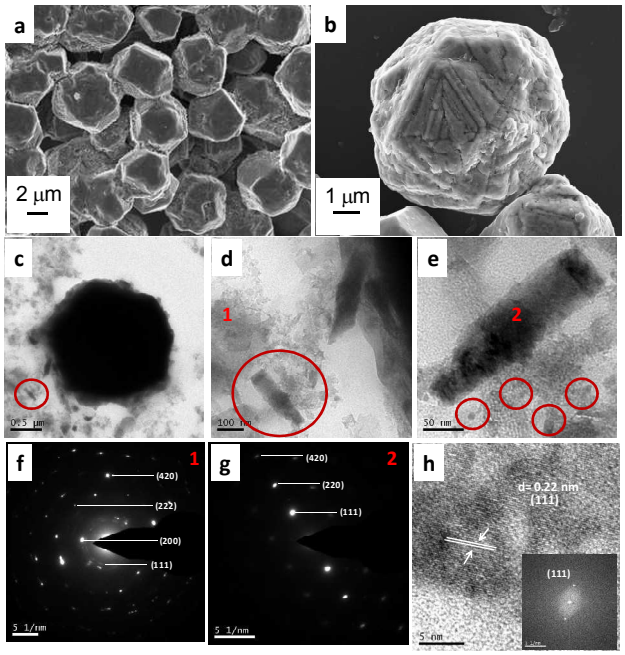

Fig. 3 (a,b) FESEM images, (c-e) TEM images, (f,g) SAED patterns and (h) HRTEM of as-prepared samples

Figure 3 (a,b) shows the FESEM images of as-prepared samples. It reveals microspheroid particles of size range 2-7 μm. From the higher magnification image of the particle it is obvious that the large number of nano-rods (50-100 nm) particles self-assembled to form microspheroid morphology (Fig. 3b). The formation of the microspheroid particles composed of nano-rod assembly has been explained shortly. The TEM image (Fig. 3c-e) reveals that how hierarchical copper microspheroid was formed through the self-assembly of copper nanorods. It was also noticed that the nanorod particles were formed via oriented growth of smaller nanoparticles (10-20 nm) (Fig. 3e). Therefore, it is pointed out that metallic copper microspheroids were formed through the self-assembly of nanoparticles with hierarchical structures. The selected area electron diffraction (SAED) pattern confirmed the polycrystalline nature (Fig. 3f) of the aggregated nanoparticles (marked as 1 in Fig. 3d), while single crystalline pattern (Fig. 3g) was noticed from nanorod particle (marked as 2 in Fig. 3e). It can be concluded that the primary smaller nanoparticles fused together with a common crystallographic orientation to form copper nanorods following "oriented attachment" growth mechanism.[42,43] Further, the nanorod particles self-assembled to form micro-spheroid morphology. The HRTEM image show the lattice fringes of copper nanoparticles with d-spacing of 0.22 nm corresponding to (111) plane (Fig. 3h), which was confirmed by FFT pattern (inset of Fig. 3h).

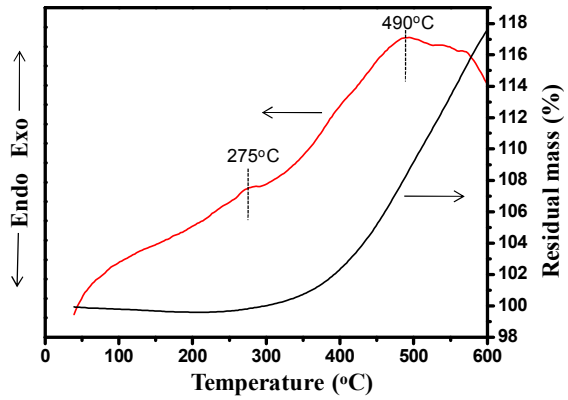

Fig. 4: DTA and TG of as-prepared Cu-nanostructure

The anti-oxidative property of Cu nanoassembly was investigated by thermogravimetry (TG) and differential thermal analysis (DTA). Figure 4 shows the DTA-TG investigation of the as-prepared Cu. TG study indicated that copper nanoassembly was stable in air up to 255°C revealing no residual mass change. In DTA analysis, two exothermic peaks were observed at about 275°C and 490°C. The first exothermic peak (275°C) was accompanied with a little amount of mass gains of 0.6% in the temperature range 255 - 310 ^{0}C. It is attributed that a very small fraction of Cu could be transformed to Cu_2O,[13,44] indicating the high stability of Cu. However, the second exothermic peak at 490°C accompanying a mass gain of 17.1% in the temperature range 310-600 ^{0}C could suggest for the oxidation of Cu to Cu_2O and/or CuO and Cu_2O to CuO. It is to be pointed out that theoretically 12.5% mass gain occurred for each conversion of Cu to Cu_2O and Cu_2O to CuO, and 25% mass gain took place for the conversion of Cu to CuO. Therefore, from the above results it indicated that the broad exothermic peak at around 490°C could be attributed to oxidations of Cu to Cu_2O and/or CuO and Cu_2O to CuO. From the above results it is clear that the synthesized product rendered excellent antioxidative property below 255°C.

To investigate the formation mechanism of the synthesized hierarchical Cu nanoassembly, time dependent solvothermal reaction was carried out at 150 °C for **75**, 90, 100, 110 and 120 mins. It was observed that Cu particles just started forming at

RSC Advances Accepted Manuscript

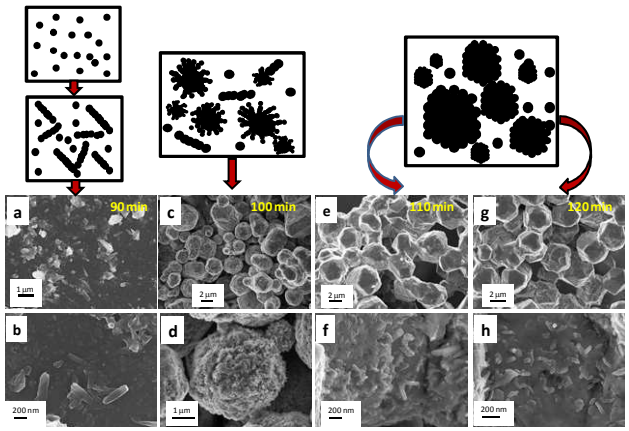

Fig. 5: Morphology evolution of the as-prepared Cu particles with increase in reaction time at 150°C

90 min of reaction time, which is evidenced from the optical images in Fig. S2 (ESI), indicating no particle formation for 75 min of reaction time (a bluish colored solution was appeared). From the XRD results, it is clear that for the reaction time 90-110 min, the as-prepared samples show the formation of metallic Cu (Fig. **S3,** ESI) as was found for 120 min reaction time (Fig. 1). The morphological evolution of the products with increase in reaction time is shown in Fig. 5. Under solvothermal condition, formamide is hydrolyzed producing formic acid and ammonia[45] following the reaction shown below. Formic acid acts as the reducing agent to convert $\mathbf{Cu^{2+}}$ to metallic Cu.

$$HCONH_2 + H_2O \rightarrow HCOOH + NH_3 \quad (1)$$

$$Cu^{2+} + 4NH_3 \rightarrow [Cu(NH_3)_4]^{2+} \quad (2)$$

$$[Cu(NH_3)_4]^{2+} + 2OH^- + HCOOH \rightarrow Cu + CO_2 + 4NH_3 + 2H_2O \quad (3)$$

The growth of the particles in solution occurs via nucleation followed by coarsening and aggregation of the primary particles. For 90 min of reaction time, the primary particles self-assembled together via oriented attachment growth mechanism to form rod-like Cu nanostructures in the presence of some aggregated copper nanoparticles. TEM images (Fig. S4, ESI) show that with increase in reaction time from 90 to 100-120 min the nanorod-like copper particles further self-assembled to each other forming copper microspheroid. It is interesting to notice that the nanorod particles were protruded onto the surface of microspheroid. However, such protrusion was becoming lower with increase in reaction time from 100 to 120 min, accordingly the aspect ratio of the nanorod was getting shorter (Fig. **S5**, ESI). The formation of microspheroid with nanorod-assembly is caused due to reduction of total energy by removing the surface energy associated with unsatisfied bonds via elimination of the solid-air or solid-liquid interfaces.[46] As a result entropy is enhanced significantly to prefer aggregation across the surface forming close-packing spheroid morphology, and thus minimizes the total surface area. The textural property of the as-prepared samples synthesized at 150°C for 120 min show BET surface area, total pore volume and average pore diameter as 0.3762 m^2g^{-1}, 0.0021 cm^3g^{-1} and 22.82 nm, respectively, which were estimated from N_2 adsorption-desorption isotherms and pore size distributions (Fig. **S6**, ESI). It is worth mentioning that the surface of copper nanoassembly was not protected by any organic coupling agent, which could protect them from oxidation. However, in the absence of any foreign protective agent, the present synthesized products exhibited remarkable antioxidative property of copper nanostructure even after 12 months exposure at ambient temperature, and up to 255°C in air.

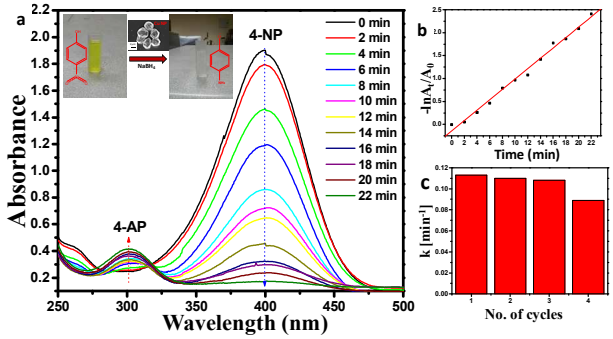

Fig. 6: (a) UV-Vis spectra for the reduction of 4-NP with 1 mg of Cu nanoassembly as catalyst, (b) pseudo-first order plot $-\ln A_t/A_o$ (Abs. intensity at 400 nm) Vs. time, (c) apparent rate constant (k) for 4 consecutive cycles.

In the present study, the catalytic efficiency of the synthesized Cu nanoassembly for the reduction of 4-NP to 4-AP in the presence of excess amount of $NaBH_4$ was investigated. 4-NP generally displays absorption spectra at 317 nm in neutral medium or acidic medium.[47] In the presence of $NaBH_4$, the absorption peak shifts to 400 nm due to deprotonation of hydroxyl group of 4-NP indicating formation of 4-nitrophenolate ion under the basic condition. The reduction of 4-nitrophenolate ion peak at 400 nm, and simultaneous increase of the absorption peak of 4-AP at 300 nm is shown in Fig. 6a. Pseudo-first order rate constant was calculated as 0.113 min^{-1} for 1 mg of catalyst at room temperature from the logarithm plot of the absorbance ($-\ln A_t/A_o$) vs reaction time (Fig. 6b). Table 1 shows the time of completion of catalytic reaction, apparent rate constant and R^2 value for different amount of catalysts. Interestingly, with increase in the catalyst amount from 1 to 3 mg, the apparent rate constant values increased from 0.113 min^{-1} to 0.279 min^{-1}, however, it was suddenly dropped to 0.239 min^{-1} for 4 mg of catalyst (Fig. S7-9, ESI). The R^2 value (close to unity) could be the good agreement with the assumption of pseudo-first-order kinetics.[23] Therefore, 3 mg catalyst was considered as optimum amount for complete catalytic reduction with highest apparent rate constant value of 0.279 min^{-1} (Fig. S10, ESI). The catalyst can be reused for at least three times with similar catalytic efficiency (Figure 6c). The catalytic efficiency of as-prepared Cu-nanoassembly was compared with that of literature

RSC Advances Accepted Manuscript

This journal is © The Royal Society of Chemistry 20xx

Table 1: Time of completion catalytic reaction, apparent rate constant (K_{app}) and R^2 value for different amount of catalysts

Sl No.	Amount of Catalysts (mg)	Time (min)	K_{app} (min^{-1})	R^2
1	1	22	0.11300	0.99015
2	2	7	0.20499	0.99340
3	3	5	0.27933	0.99316
4	4	6	0.23964	0.99557

report, and also with the reference oxides (Cu_2O and CuO) with 1 mg of catalyst each. Figures S11 and S12, ESI show (a) UV-Vis spectra and (b) pseudo-first order plots of reference Cu_2O and CuO, respectively exhibiting less catalytic efficiency than as-prepared Cu nanoassembly. The activity parameter κ (rate constant per unit gm of catalyst) of the as-prepared Cu catalyst was calculated as 113 $min^{-1}g^{-1}$, which was found to be higher than reported literature values (Table S1, ESI),[48-53] and the values for reference oxides (Table S2, ESI). It demonstrates that Cu-nanoassembly shows enhanced catalytic efficiency with faster reaction rate.

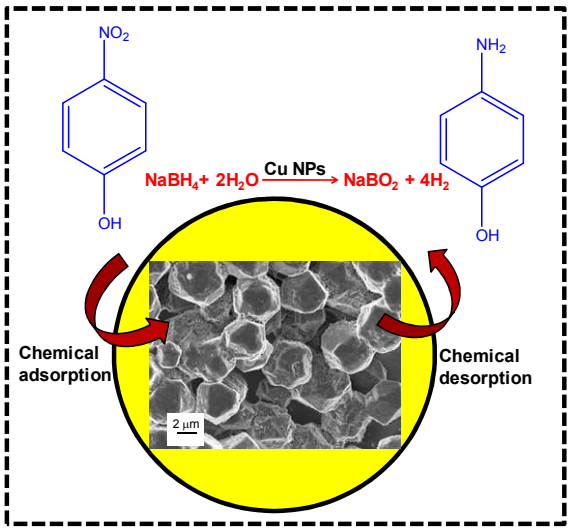

Fig. 7: Schematic representation for catalytic reaction mechanism

The catalytic reaction mechanism is shown schematically in Fig. 7. Under catalytic reaction, coadsorbtion of both the donor BH_4^- ions from $NaBH_4$ and the acceptor 4-NP molecules take place on catalyst surface (Cu-nanoassembly) ***via*** chemical adsorption.[54] However, $NaBH_4$ could transfer hydrogen species on catalytic surface under aqueous condition.[55] In this case, the Cu catalyst behaves as hydrogen shuttle for the reduction of 4-NP to 4-AP followed by desorption process.

Conclusions

In summary, hierarchical copper nanoassembly was synthesized by rapid solvothermal method at 150°C/2h in the absence of any templating agent. The nanometer size smaller particles (10-20 nm) self-assembled in a preferred orientation to form nanorod (50-100 nm) particles which further self-assembled to each other forming microspheroid-like morphology. The hierarchical copper nanoassembly without using any protective surface treatment exhibited excellent air-stability and antioxidative property due to reduced surface energy of the close packing spheroid morphology. The synthesized products showed good catalytic activities for the reduction of 4-NP to 4-AP with the apparent rate constant value of 0.279 min^{-1}. The present approach could be applicable for the synthesis of other noble metal nanostructures toward catalytic applications.

Acknowledgements

The authors acknowledge the financial support from Department of Science and Technology under DST-SERB sponsored project, GAP 0616 (Grant No.: SR/S3/ME/0035/2012), Government of India. S.G. **and P.B. are** thankful to CSIR, and R.D. and I.H.C are thankful to UGC for their fellowships.

References

1 S. Vukojevic, O. Trapp, J. D. Grunwaldt, C. Kiener and F. Schuth, *Angew. Chem., Int. Ed.,* 2005, **44**, 7978-7981.
2 Q. Darugar, W. Qian and M. A. El-Sayed, *J. Phys. Chem. B,* 2006, **110**, 143-149.
3 G. H. Chan, J. Zhao, E. M. Hicks, G. C. Schatz and R. P. Van Duyne, *Nano Lett.,* 2007, **7**, 1947-1952.
4 N. Cioffi, L. Totsi, N. Ditaranto, G. Tantillo, L. Ghibelli, L. Sabbatini, T. Bleve-Zacheo, M. D'Alessio, P. G. Zambonin and E. Traversa, *Chem, Mater.,* 2005, **17**, 5255-5262.
5 M. P. Pileni, *Nat. Mater.,* 2003, **2**, 145-150.
6 J. J. Brege, C. E. Hamilton, C. A. Crouse and A. R. Barron, *Nano Lett.,* 2009, **9**, 2239-2242.
7 I. Lisiecki and M. P. Pileni, *J. Am. Chem. Soc.,* 1993, **115**, 3887-3896.
8 B. Y. Liu, Y. Chu, Y. Zhou, L. Dong, L. Li and M. Li, *Adv. Funct. Mater.,* 2007, **17**, 933-938.
9 B. Kyun Park, S. Jeong, D. Kim, J. Moon, S. Lim and J. Sub Kim *J. Colloid interf. Sci.* 2007, **311**, 417-424.
10 N. Vilar-Vidal, M. C. Blanco, M. A. Lopez-Quintela, J. Rivas and C. Serra, *J. Phys. Chem. C,* 2010, **114**, 15924-15930.
11 N. A. Dhas, C. P. Raj and A. Gedanken, *Chem. Mater.,* 1998, **10**, 1446-1452.
12 M. Muniz-Miranda, C. Gellini, E. Giorgetti,, *J. Phys. Chem. C,* 2011, **115**, 5021-5027.
13 M. I. Dar, S. Sampath and S. A. Shivashankar, *J. Mater. Chem.,* 2012, **22**, 22418-22423.

RSC Advances Accepted Manuscript

14 F. Leung-Yuk Lam, T. Chi-Yan Martin and X. Hu, *Chem. Commun.*, 2008, 6390-6392.
15 A. Sinha, S. Kumar Das, T. V. Vijaya Kumar, V. Rao, P. Ramachandrarao, *J. Mater. Synth. Process.* 1999, **7**, 373-377.
16 H. Zhu, C. Zhang, Y. Yin, *Nanotechnology,* 2005, **16**, 3079-3083.
17 R. D. Van der Weijden, J. Mahabir, A. Abbadi, M. A. Reuter, *Hydrometallurg,* 2002, **64,** 131- 146.
18 J. Guilherme, R. Poco, R. Guardani, C. Shimmi and M. Giulietti, Mater. Res. 2006, **9**, 131-135.
19 H.‐T. Zhu, C.‐Y. Zhang, Y.‐S. Yin, *J. Cryst. Growth,* 2004, **270**, 722-728.
20 Y. Shi, H. Li, L. Chen, X. Huang, Sci. Technol. Adv. Mater. 2005, **6**, 761–765.
21 H. Kawasaki, Y. Kosaka, Y. Myoujin, T. Narushima, T. Yonezawa and R. Arakawa, *Chem. Commun.,* 2011, **47**, 7740-7742.
22 Y. Wei, S. Chen, B. Kowalczyk, S. Huda, T. P. Gray and B. A. Grzybowski, *J. Phys. Chem. C,* 2010, **114**, 15612-15616.
23 P. Deka, R. C. Deka and P. Bharali, *New J. Chem.,* 2013, **37**, 2399-2407.
24 Z. Dong, X. Le, Y. Liu, C. Dong and J. Ma, *J. Mater. Chem. A,* 2014, **2**, 18775-18785
25 T. Bhowmik, M. K. Kundu and S. Barman, *RSC Adv.,* 2015, **5**, 38760–38773.
26 M. Rocha, C. Fernandes, C. Pereira, S. L. H. Rebelo, M. F. R. Pereira and C. Freire, *RSC Adv. (2015),* DOI: 10.1039/C4RA15865B.
27 A. K. Patra, A. Dutta and A. Bhaumik, *Catal. Commun.*,2010, 11, 651-655.
28 A. Dutta, A. K. Patra and A. Bhaumik, Micropor. Mesopor.Mater. 2012, 155, 208-214.
29 Q. Hua, T. Cao, X-K. Gu, J. Lu, Z. Jiang, X. Pan, L. Luo, W-X. Li and W. Huang, *Angew. Chem.*, 2014, 53, 4856-4861.
30 M. Zhu and G. Diao, *Catal. Sci. Technol.*, 2012, 2, 82-84.
31 Y. Feng and X. Zheng, *Nano Lett.,*2010, 10, 4762-4766.
32 P. W. Park, J. S. Ledford, *Appl. Catal. B,* 1998, 15, 221-231.
33 K. Soni, B. S. Rana, A. K. Sinha, A. Bhaumik, M. Nandi, M. Kumar and G. M. Dhar, *Appl. Catal. B: Environ.*, 2009, 90, 55-63.
34 R. Xu, H. C. Zeng, *Langmuir,* 2004, 20, 9780-9790.
35 J. J. Teo, Y. Chang and H. C. Zeng, *Langmuir,* 2006, 22, 7369-7377.
36 M. Konsolakis, S. A.C. Carabineiro, E. Papista, G. E. Marnellos, P. B. Tavares, J. A. Moreira, Y. Romaguera-Barcelay and J. L. Figueiredo, *Catal. Sci. Technol.,* 2015, 5, 3714-3727.
37 W. Wang, G. Wang, X. Wang, Y. Zhan, Y. Liu and C. Zheng, *Adv. Mater.* 2002, 14, 67-69.
38 Y. Zhang, I. J. Drake and A. T. Bell, Chem. Mater., 2006, 18, 2347-2356.
39 Z. Zhang, H. Che, Y. Wang, J. Gao, X. She, J. Sun, Z. Zhong and F. Su, RSC Adv., 2012, 2, 2254-2256.
40 J. Y. Kim, J. A. Rodriguez, J. C. Hanson, A.I. Frenkel and P. L. Lee, *J. Am. Chem. Soc.*, 2003, 125, 10684-10692.
41 G. Derrien, C. Charnay, J. Zajac, D.J. Jones and J. Roziere, Chem. Comm., 2008, 3118-3120
42 S. Ghosh and M. K. Naskar, *RSC Adv.,* 2013, 3, 4207-4211.
43 R. L. Penn and J. F. Banfield, *Science,* 1998, 281, 969-971.
44 W. Hu, L. Zhu, D. Dong, W. He, X. Tang and X. Liu, *J. Mater. Sci: Mater Electron,* 2007, 18, 817-821.
45 B. Wang and Z. Cao, *J. Phys. Chem. A,* 2010, 114, 12918-12927.
46 R. L. Penn, *J. Phys. Chem. B,* 2004, 108, 12707-12712.
47 Z. Jin, M. Xiao, Z. Bao, P. Wang and J. Wang, *Angew. Chem., Int. Ed.,* 2012, 51, 6406-6410.
48 J. Pal, C. Mondal, A. K. Sasmal, M. Ganguly, Y. Negishi and T. Pal, *ACS Appl. Mater. Interfaces*, 2014, 6, 9173−9184.
49 T. R. Mandlimath, B. Gopal, *J. Mol. Catal. A: Chem*., 2011, 350, 9-15.
50 M. H. Rashid, T. K. Mandal, *J. Phys. Chem. C,* 2007, 111, 16750 - 16760.
51 S. Tang, S. Vongehr and X. Meng, *J. Phys. Chem. C,* 2010, *114,* 977–982
52 Z. Jiang, J. Xie, D. Jiang, X. Wei and M. Chen, *CrystEngComm* , 2013, 15, 560–569.
53 H. -L. Jiang, T. Akita, T. Ishida, M. Haruta and Q. Xu, *J. Am. Chem. Soc.* 2011, 133, 1304–1306.
54 Z. Jiang, J. Xie, D. Jiang, X Wei and M. Chen, *CrystEngComm,* 2013, 15,560-569.
55 R. Das, S. Ghosh, I. H. Chowdhury and M. K. Naskar, *New J. Chem*.,(2015), DOI:10.1039/c5nj02088c.

RSC Advances Accepted Manuscript

This journal is © The Royal Society of Chemistry 20xx

Graphical Representation

Hierarchical copper nanoassembly was synthesized by solvothermal treatment at 150 °C/2h in the absence of any templating agents, which exhibited excellent air-stability, antioxidative property and catalytic reduction of 4-nitrophenol.

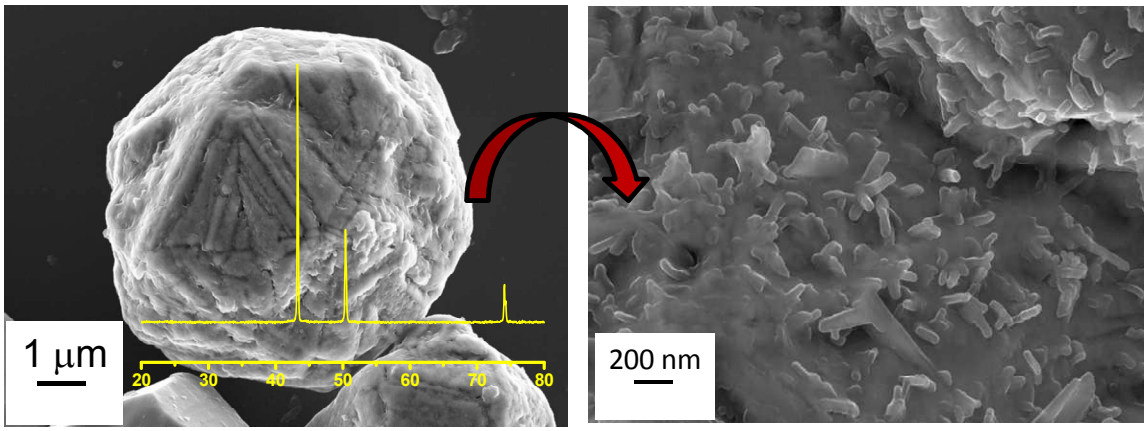

RSC Advances Accepted Manuscript